DNA, sugars, and proteins at work in optics

Koen Clays
Department of Chemistry, University of Leuven, Celestijnenlaan 200D, B-3001 Leuven, BELGIUM
and
Department of Physics and Astronomy, Washington State University, Pullman, WA, USA

ABSTRACT

In this Keynote presentation, we will review the use of selected biosystems in relevant optical applications:

Complementary DNA strands can be used to put chromophore couples, *e.g.* for energy transfer between donor and acceptor, at a desired distance. By using the appropriate oligonucleotide length, we have spaced donor and acceptor at the Förster distance to show the influence of a carefully designed photonic bandgap on the Förster resonant energy transfer (FRET) efficiency.

Amylose can be used to optimize the conformation of extended chromophores. Long conjugated systems show enhanced optical properties, but only in the *all-trans* conformation. This unlikely situation has been enforced by including the elongated molecule as a guest in the amylose host. The theoretically predicted enhancement in nonlinear optical polarizability, linear with conjugation length, has been demonstrated, but only when the chromophore was in the amylose.

Fluorescent proteins can be used in cellular imaging. We will focus on the recent development (by genetic engineering) and characterization (by hyper-Rayleigh scattering) of fluorescent proteins for combined multiphoton fluorescence and second harmonic imaging. A small rainbow of fluorescent proteins has been characterized for their nonlinear optical properties.

Keywords: DNA, energy transfer, photonic bandgap, photonic crystal, amylose, chromophore, conformation, fluorescent proteins

1. INTRODUCTION

A number of applications of linear and nonlinear optical effects require the precise control of the position of active elements at the nanometer scale. Other optical effects are strongly influenced by conformational changes of the chromophore, or by molecular interactions with the surrounding of the active element. These effects also occur at the nanometer scale. Optical effects and molecular interactions are strongly influenced by nanometer scale effects, because of the inherent dimensions of molecules and optical wavelengths. Biological materials are also structured at the nanometer scale. The fundamental building stones of biological materials are nanometer-sized amino acids; nucleotides; and monosaccharides, leading to proteins; DNA; and functional carbohydrates, *respectively*. It is possible to couple optical functionality with biological material. A prototypical example from nature is bacteriorhodopsin, where the precise positioning of a chromophore for photon absorption and a proton channel can lead to a membrane potential. More recently, a complete rainbow of fluorescent proteins has been engineered. The different colors for absorption and emission have been induced by controlling the size of the chromophore and the nature of the interactions between the chromophore and the protein surrounding on the nanometer scale. In this Keynote presentation, we will give three examples of how an optical effect has been optimized by coupling it to biological structural elements, to be able to control interaction or conformation at the nanometer scale.

Nanobiosystems: Processing, Characterization, and Applications V, edited by
Norihisa Kobayashi, Fahima Ouchen, Ileana Rau, Proc. of SPIE Vol. 8464, 84640M
 · doi: 10.1117/12.928837

2. OPTIMIZING THE EFFICIENCY OF FÖRSTER RESONANT ENERGY TRANSFER

Förster Resonant Energy Transfer (FRET) is a non-radiative form of energy transfer, mainly between singlet states, based on Coulombic, hence, long-range, interaction between the excited state of a donor molecule and the ground state of an acceptor molecule. Light energy is absorbed by the donor molecule having an absorption band at higher energy than the acceptor molecule. The excited state of the donor molecule can relax to the ground state by a number of mechanisms. If a molecule with an absorption spectrum showing appreciable overlap with the emission spectrum of the donor (hence an absorption spectrum at lower energy than that of the donor molecule) is in the neighborhood of the donor, energy can be transferred by long-range Coulombic non-radiative interaction to this acceptor molecule. This is then an additional relaxation pathway, in competition with the other pathways, such as direct emission of a photon by the donor molecule. For efficient energy transfer, the latter is a loss mechanism, since the energy of the emitted photons is not transferred to and captured by the acceptor molecule.[1]

To enhance the efficiency of the energy transfer, any possible loss mechanism has to be avoided. Since direct emission by the donor molecule is such a loss mechanism, any way to suppress this emission is expected to enhance the FRET efficiency. One way to suppress emission is by engineering a photonic bandgap with a spectral overlap with the emission band.[2,3] To study the effect of the presence of such a photonic bandgap on the FRET efficiency, we have controlled the overlap integral between donor emission and acceptor absorption by selecting a particular donor-acceptor couple (Cy3-Cy5, Figure 1) and by fixing the distance between the donor and the acceptor.

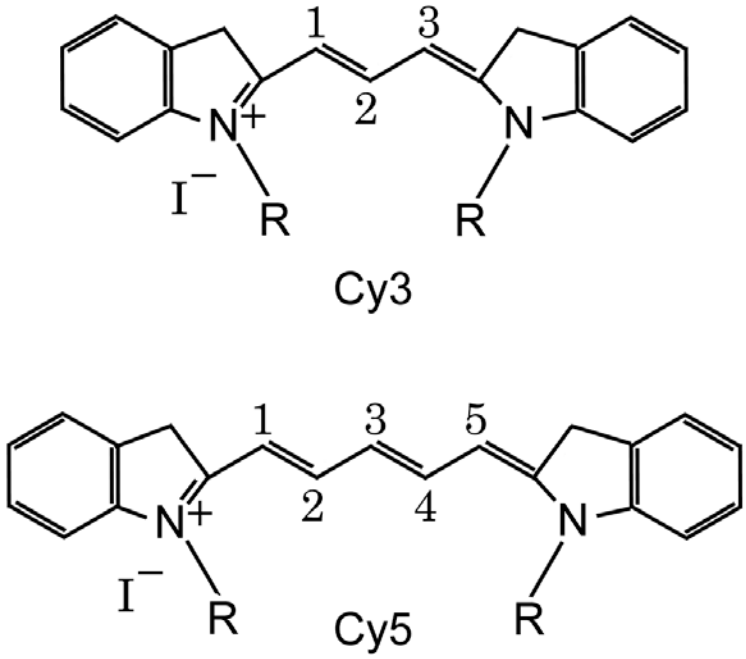

Figure 1. Molecular structure of the cyanine dyes Cy3 (energy donor dye) and Cy5 (energy acceptor dye) used in this study.

To have the largest sensitivity for the photonic bandgap effect, this distance was selected to be the Förster distance, at which the FRET efficiency is at 50% of its maximum. For the Cy3-Cy5 couple, this distance is approximately 5 nanometer. This was realized by linking these dyes to the opposite ends of 2 complementary single-stranded DNA linkers of 17 nucleotides, (17T)-Cy5 and Cy3-17(A). The distance between base-pairs in DNA is 0.3 nanometer, resulting in the correct distance between the donor and the acceptor dye after annealing the complimentary oligonucleotides. The FRET efficiency was estimated from the integrated emission band intensities for donor and acceptor. In solution (TRIS buffer, pH 8), this efficiency was, depending on the ionic strength, between 38 and 45% (Figure 2).

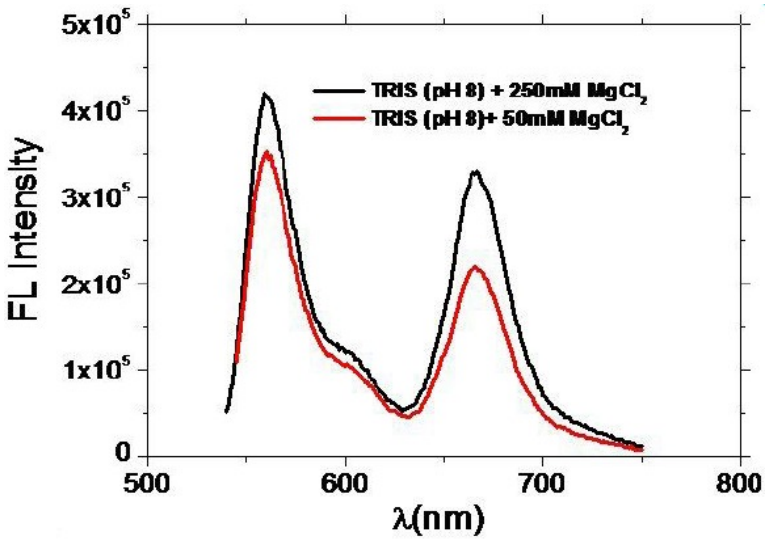

Figure 2. Fluorescence spectra of double-stranded oligonucleotides with Cy3-Cy5, excited at 535 nm in solution.

This solution was now used for infiltrating the air voids in an FCC photonic crystal of monodisperse and spherical silica particles. Two sizes of particles have been used. One small size (208 nm) was used to create a photonic bandgap out of all spectral regions of interest (450 nm, to the blue of the absorption band of the donor). One size was chosen (272 nm) to result in a photonic bandgap exactly overlapping with the emission band of the donor (600 nm, see Figure 3). Since donor-acceptor couple and distance were constant, any change in the FRET efficiency should be traced to the photonic bandgap difference.

For the control crystal with its bandgap not overlapping with the emission spectrum of the donor, the FRET efficiency was 37%, while for the active crystal with its bandgap overlapping with the emission spectrum of the donor, the FRET efficiency was 61% (Figure 4). This increase was induced by the photonic bandgap effect, another nanometer size effect at the optical range. But the emphasis in this context is on the precise control of the distance by the use of oligonucleotides.

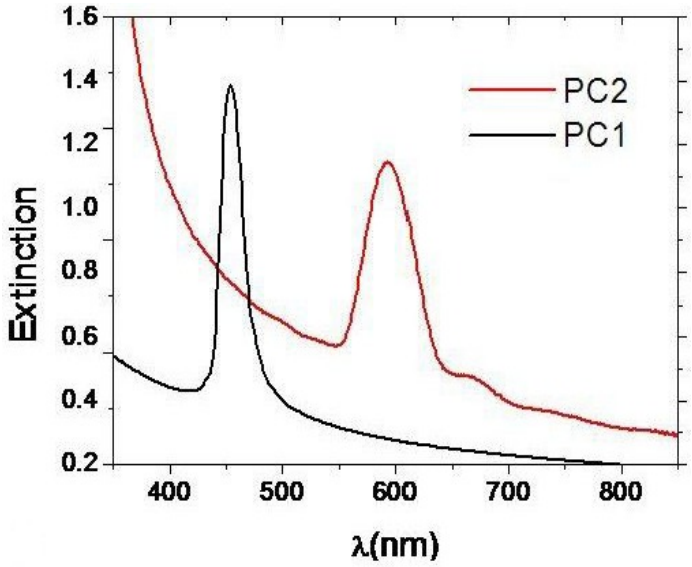

Figure 3. Extinction spectra of the reference photonic crystal (black) with its photonic bandgap out of the spectral region of interest and of the active photonic crystal (red) with its photonic bandgap overlapping with the emission spectrum of the donor.

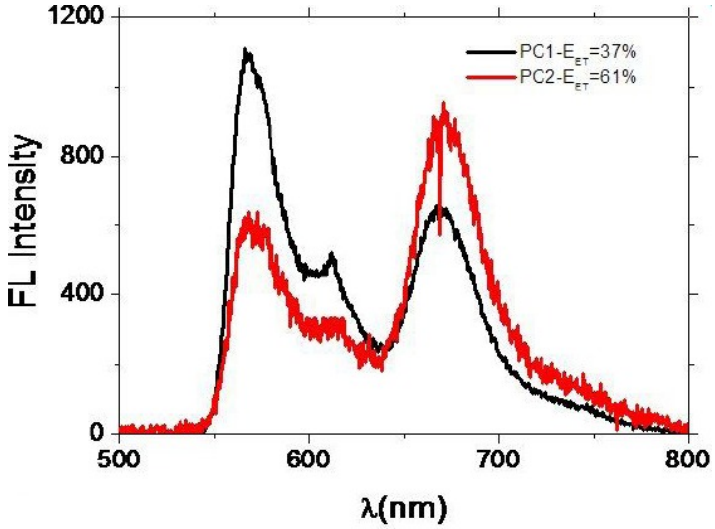

Figure 4. Fluorescence spectra of double-stranded oligonucleotides with Cy3-Cy5, excited at 535 nm in solution, in the reference photonic crystal (black) with its photonic bandgap out of the spectral region of interest and in the active photonic crystal (red) with its photonic bandgap overlapping with the emission spectrum of the donor.

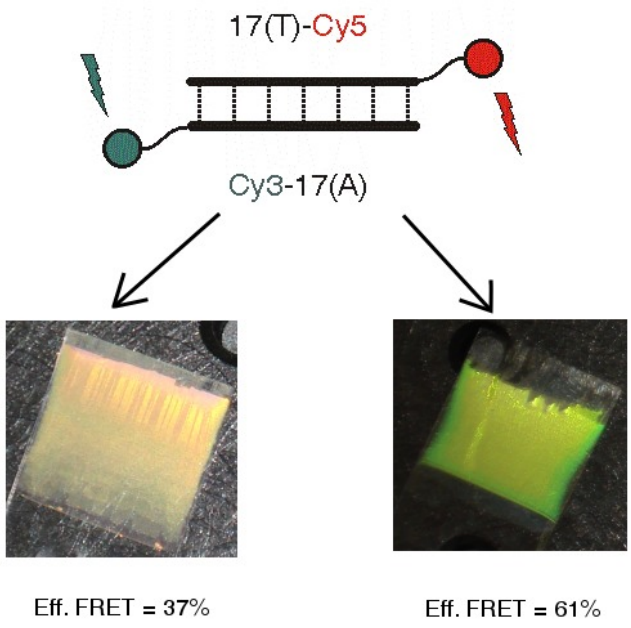

Figure 5. Schematic representation of the DNA construct with complementary oligonucleotides attached to the donor Cy3 and acceptor Cy5, with a photograph of the resulting acceptor emission from the reference photonic crystal (left) and of the enhanced emission from the acceptor in the active photonic crystal suppressing the emission of the donor (right).

3. OPTIMIZING THE CONFIGURATION OF CHROMOPHORES FOR SECOND-ORDER NONLINEAR OPTICAL APPLICATIONS BY INCLUSION IN AMYLOSE

For second-order nonlinear optical applications, such as frequency-doubling, electro-optic modulation, or terahertz radiation generation, noncentrosymmetry is essential, as for any even-order nonlinear effect. Yet to optimize the nonlinear optical response in general, be it for linear, even- or odd-order nonlinear optics, the number of polarizable electrons is also crucial. In organic chromophores, this number translates in the length of the conjugated pi-systems, since pi-electrons are much more loosely bound and therefore much more polarizable.[4] But for a large effect, this conjugated system should be in the *all-trans* configuration. For longer conjugated systems, this is not necessarily the case.

We had studied the influence of the length of the conjugated bridge between a donor and an acceptor molecule to induce the noncentrosymmetry. We had found limiting or saturation behavior at very short conjugation lengths, in spite of theoretical predictions for linear enhancement with number of ethylene units in the *all-trans* configuration, at least for up to the decapentaenylene bridge. Theory also confirmed that *cis*-configurations result in lower second-order nonlinear optical response.[5]

To try to induce the optimal *all-trans* configuration, the inclusion of the chromophore within the interior of an amylose helix was envisaged, to enforce a linear configuration. Amylose was chosen because of its nanometer dimensions that are ideally suited for this purpose. For the short dimethylaminostilbazolium (DAST) benchmark, an enhancement in molecular second-order nonlinear optical response by a factor of two had been observed.[6]

A matrix of a number of amylose molecular weights and hemicyanine chromophores with different conjugation lengths (from ethylene over butadienylene, hexatrienylene, octatetraenylene, to decapentaenylene) was used to study the effect.

Although the particular nature of the amylose plays an important role, the predicted enhancement of an order of magnitude with respect to the DAST benchmark (factor of two for the amylose inclusion and factor of five for going from ethylene to decapentaenylene) was indeed observed.[7]

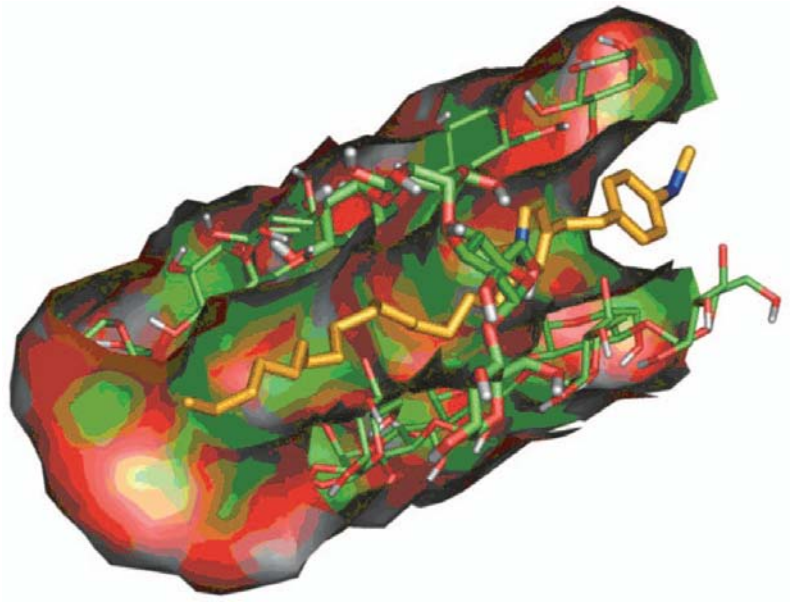

Figure 6. Schematic representation of the inclusion complex between a hemicyanine chromophore as guest molecule and an amylose helix as docking host.[7]

4. FLUORESCENT PROTEINS FOR SECOND-HARMONIC IMAGING

Second-harmonic imaging (SHIM), or second-harmonic generation (SHG) microscopy, is a new imaging technique that is highly complementary to two-photon fluorescence.[8,9] Technically, it requires the same pulsed near-infrared laser as two-photon fluorescence does, with only an additional detection path in the forward direction with separate optical filtering around the second-harmonic wavelength.[10] But the additional structural information that is obtained is highly valuable. While two-photon fluorescence, being a third-order nonlinear optical (NLO) effect, is originating in all structures, the second-harmonic signal, being a second-order NLO effect, is only observed for non-centrosymmetric arrangements of the chromophores.[11,12] To improve the detection efficiency, a multifocus scanning technique has been implemented and used in cardiology.[13] The physical origin of the second-harmonic signal from endogenous proteins has been attributed to their dipolar and chiral non-centrosymmetric nature.[14] Several works have reported on the qualitative use of second-harmonic imaging from green fluorescent protein, GFP.[15,16]

We have recently reported a quantitative value for the second-order NLO properties for Enhanced Green Fluorescent Protein (EGFP) and for the photoswitchable variant Dronpa.[17] This work has shown that the chromophore in this GFP is capable of generating a second-harmonic signal, which could be used for second-harmonic imaging. With the availability of a rainbow of fluorescent proteins (FPs),[18] we have previously extended this work to screen first a set of three variants, namely EGFP as a benchmark, and enhanced Yellow FP (EYFP) and DsRed.[19] It was found that while the linear optical properties, *i.e.*, the absorption and emission spectrum, show the gradual trend from green over yellow to red upon extending the chromophore through pi-interaction and larger conjugation, the second-order NLO properties do not follow this trend. The smallest second-order NLO response had been observed for EYPF. This striking observation had been rationalized in terms of the effective symmetry of the actual chromophore.[19]

We have then extended this series towards the red, with the FP variants mStrawberry and mCherry.[20] The observation of the continuously increasing hyperpolarizabilities upon red shifting has confirmed the previously observed trend. This work had also pointed out that these newer variants should perform better for SHIM applications because of the larger one- and two-photon resonance enhancement that can be achieved.[20] We have now complemented this study with a yellow variant, zFP538, which, unlike EYFP, does obey the trend. The contrasting observations between linear optics (similar yellow absorption and emission) and second-order nonlinear optics (small hyperpolarizability in EYFP, larger and in between EFGP and DsRed for zFP538) show how genetic engineering guidelines to design optical properties should take into account symmetry arguments when trying to optimize second-order NLO properties.

4.1 Materials and Methods

The proteins were expressed and purified as described previously.[17,19-21] After HPLC affinity purification, the samples were dialyzed against a 20mM HEPES buffer containing 150 mM NaCl at a pH of 7.5. The pRSET plasmids containing the mCherry and mStawberry gene were a generous gift from Roger Y. Tsien's lab. The proteins were checked for purity by SDS-PAGE and mass spectrometry. Concentration of the samples was determined using the extinction coefficient of the chromophore at the wavelength of maximal absorption.[22] The nonlinear optical experiments were carried out starting from 100 μM protein solutions.

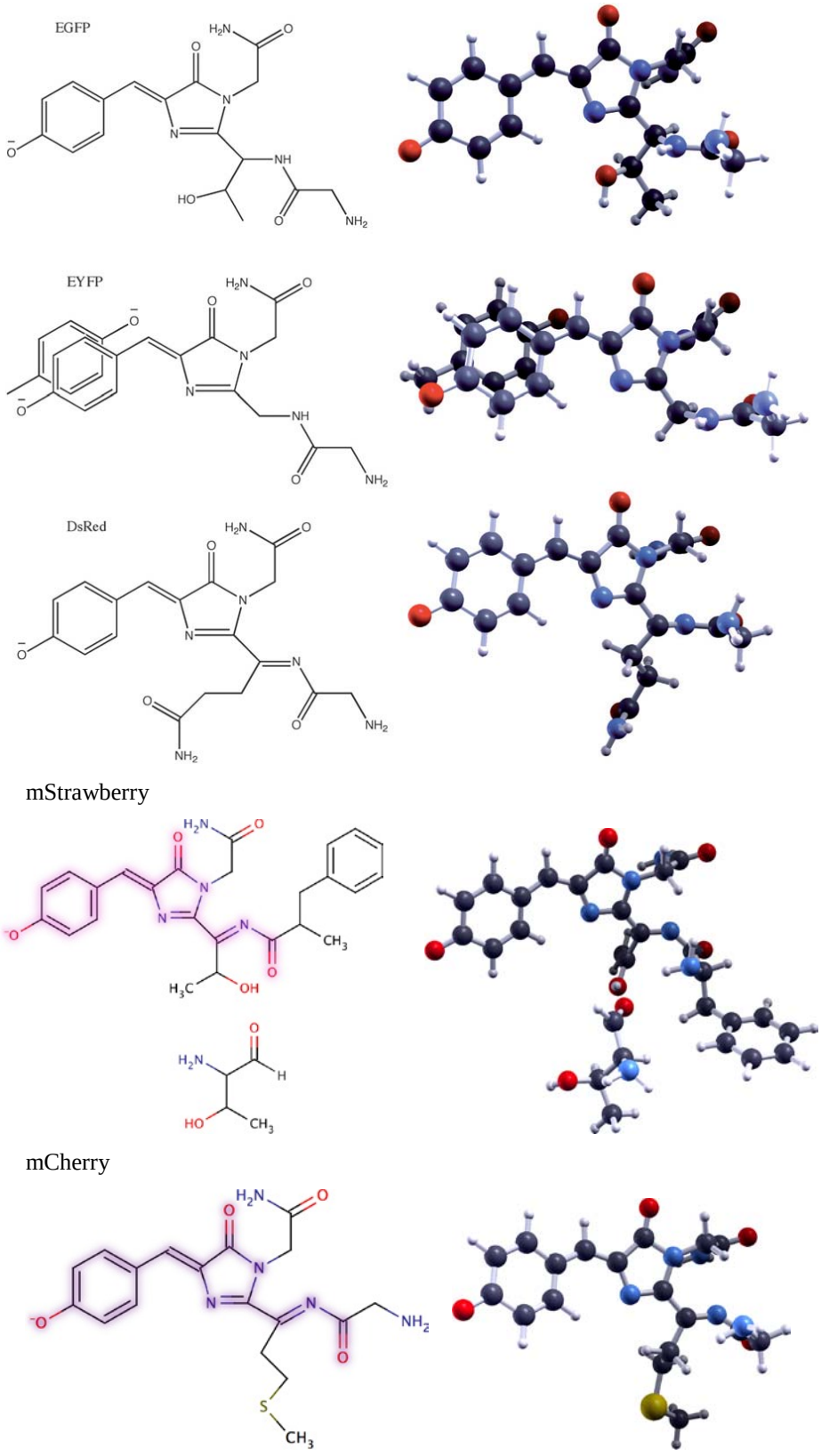

Figure 7. Models of the isolated EGFP, EYFP, DsRed[19] mStrawberry and mCherry[20] chromophores.

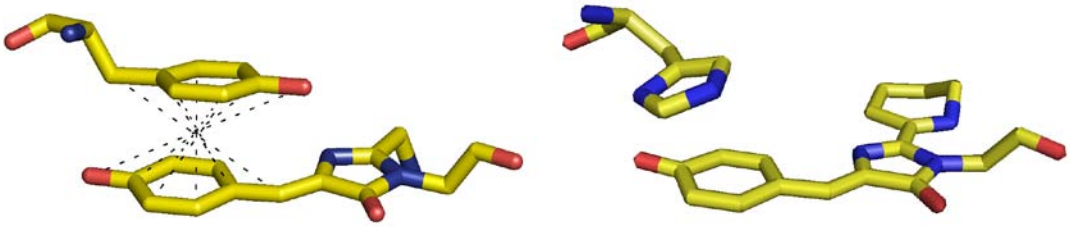

Figure 8. Models of the stacking interaction between tyrosine-66 chromophoric moiety and phenolic residue of tyrosine-203 in EYFP (left)[20,23] and between this tyrosine and histidine in zFP538 (right).

The linear optical characterization was performed on commercially available instruments. The absorption spectra were obtained on a Perkin Elmer Lambda 900 UV/Vis spectrometer. The fluorescence spectra were obtained with an Ocean Optics setup, consisting of a 430 nm LED (Kingbright L53MBC) with appropriate filter and focusing lens for the excitation. The emitted light was collected at a 90° angle using a fiber (Ocean Optics QP400-2-VIS/BX) fitted with a collimating lens (Ocean Optics 74-UV) and detected by a charge coupled device (CCD) spectrometer (Ocean Optics USB4000).

For the experimental determination of the second-order nonlinear polarizability, or first hyperpolarizability β, of proteins, only hyper-Rayleigh scattering (HRS) can be used.[24] But for the applicability of this incoherent second-order nonlinear scattering technique, it is essential to discriminate between the signal coming for the second-order scattering, and the signal coming for two-photon fluorescence, a third-order nonlinear contribution. In the spectral domain, it is not possible to make the distinction, since a narrow HRS signal at the second-harmonic wavelength is superimposed on the broad multiphoton spectrum.[25] Therefore, we have employed an amplitude-modulation (AM) frequency-resolved technique, to show whether or not there is a multiphoton fluorescence contribution at the second-harmonic wavelength in the first place, and if so, to deduce an accurate, fluorescence-free hyperpolarizability value.[26,27] This approach is the Fourier-transform in the frequency-domain of the more intuitive separation between immediate (hyper-Rayleigh) scattering and time-delayed (multi-photon) fluorescence in the time domain.[28] We use the intrinsic high harmonic content of an ultra short laser pulse and cross-correlation electronics to extract the amplitude and phase of the HRS response at successive higher AM frequencies. Any fluorescence contribution, characterized by a finite response time, shows up as demodulation for high frequencies. This shows up as a reduction of the apparent frequency-dependent hyperpolarizability, with an inflection point at the AM frequency corresponding with the inverse of the fluorescence lifetime. The high-frequency limit of the apparent β is the accurate, fluorescence-free β value. As an additional sign of the contribution of the delayed fluorescence, a growing phase shift between a scattering reference and the HRS signal is observed. The simultaneous fitting of the amplitude and phase data ensures a precise estimate of the fluorescence-free hyperpolarizability, in addition to estimates for the fluorescence contribution and lifetime.[27] This technique has been shown to be useful to deduce the β values of a large number of fluorescent chromophores,[4-8,29-34] including fluorescent proteins.[17,19,20]

4.2 Results

The linear optical absorption spectra of the series of FPs are shown in Figure 9. These spectra nicely show the smooth progression in wavelength of maximal absorption, $\lambda_{max,abs}$, tabulated in Table 1. Also clearly observable is the much narrower absorption peak for EYFP, a clear indication of the stacking interaction that is causing the red shift in the absorption and the emission with respect to the benchmark green EGFP. This stacking is resulting in an effectively larger conjugated system. These linear optical properties are in line with the expectations for these FPs[18,22] and confirm the presence and the nature of the chromophore inside the protein pocket.

As for the nonlinear optical properties, determined by frequency-resolved femtosecond hyper-Rayleigh scattering, all proteins exhibit, as expected,[17,20] multiphoton fluorescence in concurrence with hyper-Rayleigh scattering, necessitating the simultaneous fitting of demodulation and phase data towards the high-frequency fluorescence-free hyperpolarizability value, $\beta_{HRS,800}$; a multiphoton fluorescence contribution, $\chi_{flu,800}$; and a fluorescence lifetime, τ_{flu}.[27] This is exemplified in Figure 10, showing the frequency dependence of the apparent hyperpolarizability value and phase for the zFP protein at 800 nm.

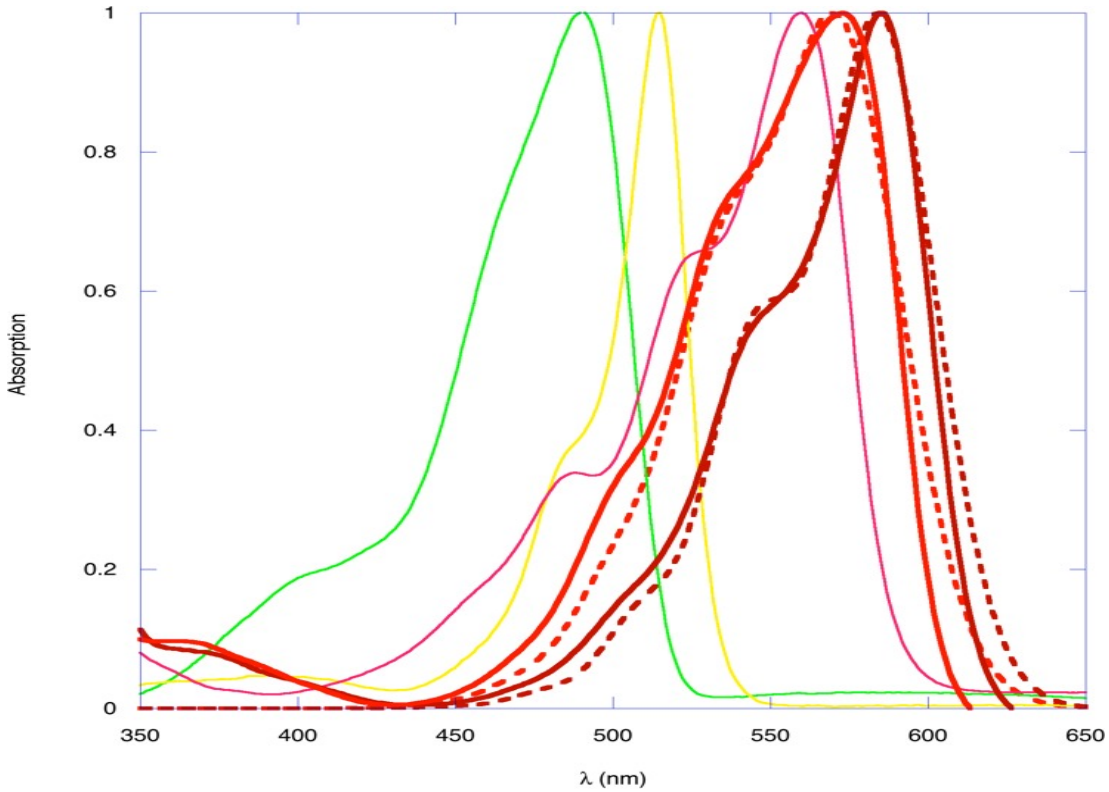

Figure 9. Experimental absorption spectra for (from left to right) EGFP (green line); EYFP (yellow line); DsRed (pink line); mStrawberry (light red); and mCherry (dark red). The dashed lines are simulated spectra for mStrawberry and mCherry.[20]

Table 1. Linear and nonlinear optical properties of fluorescent proteins investigated: wavelength of maximal absorption, $\lambda_{max,abs}$; wavelength of maximal fluorescence, $\lambda_{max,flu}$; experimentally determined first hyperpolarizabilities, $\beta_{HRS,800}$; derived static hyperpolarizability, $\beta_{HRS,o}$; multiphoton fluorescence contribution, $\chi_{flu,800}$; and fluorescence lifetime, τ_{flu}.

	EGFP	EYFP	zFP538	DsRed	mStrawberry	mCherry
$\lambda_{max,abs}$ (nm)	488	513	528	558	575	587
$\lambda_{max,flu}$ (nm)	507	527	538	583	596	610
$\beta_{HRS,800}$ (10^{-30} esu)	107 ± 17	49 ±5	90 ± 5	81 ± 8	104 ±5	134 ± 16
$\beta_{HRS,o}$ (10^{-30} esu)	33 ± 5	18 ± 2	38 ± 2	39 ± 4	54 ± 3	71 ± 8
$\chi_{flu,800}$ (10^{-30} esu)	137 ± 12	53 ± 6	120 ± 15	103 ± 7	117 ± 6	120 ± 20
τ_{flu} (ns)	1.0 ± 0.4	1.5 ± 0.6	2.6 ± 0.8	1.2 ± 0.4	1.0 ± 0.1	1.1 ± 0.1

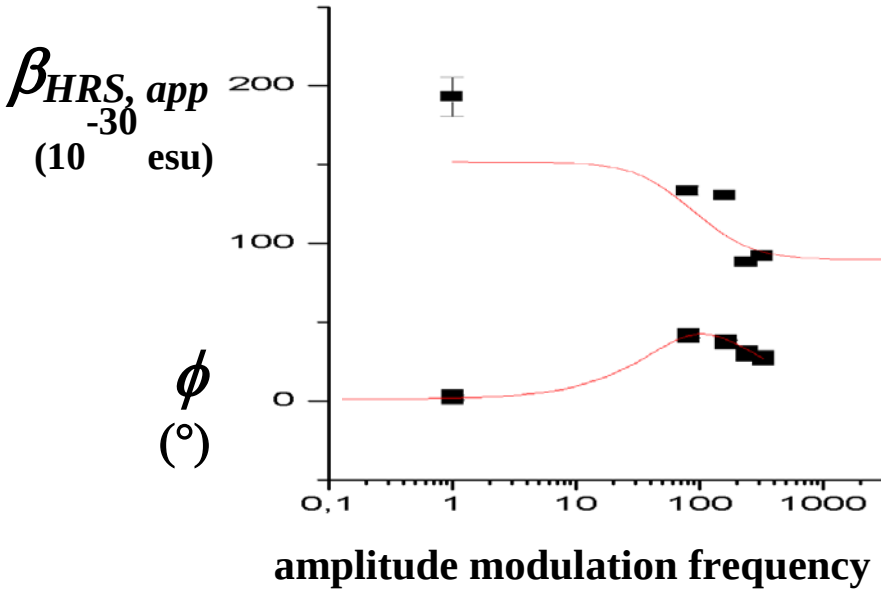

Figure 10. Apparent, amplitude modulation frequency dependent, dynamic (800 nm) first hyperpolarizability, $\beta_{HRS,app}$, and phase difference ϕ between total HRS signal and signal from pure scattering reference, for zFP538 protein.

Fluorescence-free hyperpolarizability values are extracted as the high-frequency limiting values of the demodulated values, based on the assumption of a single-exponential decay of the fluorescence. Because of the electronic resonance induced by the absorption between the fundamental laser wavelength (800 nm) and the second-harmonic wavelength (400 nm), there is considerable resonance enhancement of the optical properties. In particular, the second-order nonlinearity is affected by both one- and two-photon resonance enhancement. Based on a simple two-level model.[35] it is possible to correct for this effect and deduce a corrected, resonance-free, wavelength-independent value for the static hyperpolarizability, $\beta_{HRS,o}$, or the limit for infinitely long wavelength. These values are also tabulated in Table 1, and graphically represented in Figure 11, together with the wavelengths of maximal absorption and emission, $\lambda_{max,abs}$ and $\lambda_{max,flu}$,*respectively*.

From theory, a larger first hyperpolarizability is expected for a smaller energy difference between HOMO and LUMO for the chromophore, congruent with a longer wavelength of maximal absorption. Hence, the largest static hyperpolarizability is expected for mCherry with its longest wavelength of maximal absorption and emission. This is also observed. From Figure 11, it is clearly observed that there is indeed a similar trend for the wavelengths of maximal absorption and emission as for the first hyperpolarizabilities corrected for resonance effects. The striking observation is, however, how the two different kinds of stacking, shown in Figure 8 for EGFP and for zFP538, resulting in very similar ***linear*** optical properties (triangles for both FPs are essentially overlapping), induce a very different ***second-order nonlinear*** optical response. The first hyperpolarizability value for zFP538 is twice as large as the value for EGFP.

We had conjectured that the anomalously low value for the first hyperpolarizabiltiy of EGFP was due to the centrosymmetric nature of the stacking[19,23] indicated in the left part of Figure 8. This strategy is not the simple enlargement of the conjugation in the chromophore, since the chromophore itself is identical for EGFP and EYFP. The shift to longer absorption and emission wavelength had been attributed to the π–π stacking between the chromophore phenolic ring (from Tyrosine-66) and the residue of Tyrosine-203.[19] While this induced a larger effective polarizable system, a sufficient condition for longer wavelength absorption and emission, it also introduces an inversion centre for part of the effective chromophore, namely in between the two phenolic moieties. Since for second-order nonlinear effects, centrosymmetric structures do not contribute, this results in an effectively shorter chromophore as far as any second-order nonlinear effects are considered. Now, with the additional experimental result of a signficantly larger value for the hyperpolarizability of zFP538, showing similar stacking, yet with histidine, and, hence, without the centrosymmetry, and which is in addition nicely in line with the hyperpolarizability values of the other FPs, our conjecture is strongly corroborated.

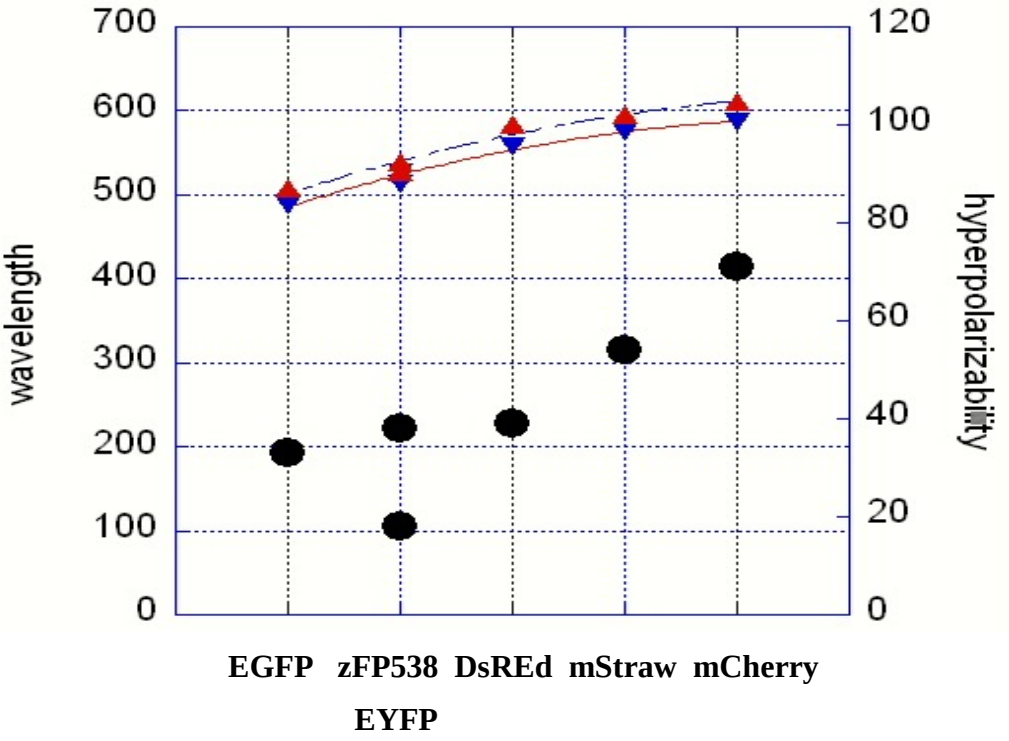

Figure 11. Graphical representation of linear optical properties (wavelength of maximal absorption, $\lambda_{max,abs}$, blue triangles down; and wavelength of maximum fluorescence, $\lambda_{max,flu}$, red triangles up, left ordinate axis; units of nm, lines show the continuous trend) together with second-order nonlinear optical property (resonance-free static first hyperpolarizability, $\beta_{HRS,o}$, solid circles ●, right ordinate axis, units of 10^{-30} esu).

5. CONCLUSIONS

In this Keynote presentation, we have reviewed three examples of how an optical effect has been optimized by coupling it to biological structural elements, to be able to control interaction or configuration at the nanometer scale. We have shown how DNA can be used to put a donor-acceptor couple at a specific distance in energy transfer studies. We have shown how amylose can impose the optimal *all-trans* configuration on hemicyanine dyes with long conjugation lengths. Finally, we have shown that symmetry arguments disrupt the trend in the second-order nonlinear optical properties of fluorescent proteins. While stacking, irrespective of symmetry, is sufficient to induce a red shift in their linear optical properties, its consequence on the second-order nonlinear polarizability is highly dependent on the symmetry of this stacking. Centrosymmetric stacking has a detrimental effect on the value of the first hyperpolarizability in EYFP, while non-centrosymmetric stacking as in zFP538 results in a value for the hyperpolarizability that is in line with the expectations based on frontier orbital energy (or absorption wavelength) arguments.

6. REFERENCES

[1] Kolaric, B., Baert, K., Vallée, R. A. L., Van der Auweraer, M. and Clays, K., "Controlling the Fluorescence Resonant Energy Transfer by Photonic Crystal Bandgap Engineering", Chem. Mat. **19**(23), 5547-5552 (2007).

[2] Song, K., Vallée, R. A. L., Van der Auweraer, M. and Clays, K., "Fluorophores-modified silica sphere as emission probe in photonic crystals", Chem. Phys. Lett.**421**, 1-4 (2006).

[3] Baert, K., Song, K., Vallée, R. A. L., Van der Auweraer, M. and Clays, K., "Spectral Narrowing of emission in self-assembled colloidal photonic superlattices", J. Appl. Phys. **100**(12), 123112 (7 pages) (2006).

[4] Clays, K., Hendrickx, E., Verbiest, T. and Persoons, A., "Nonlinear Optical Properties of Correlated Chromophores in Organic Superstructures", Adv. Mat. **10**(9), 643-655 (1998).

[5] Clays, K., Wostyn, K., Olbrechts, G., Persoons, A., Watanabe, A., Nogi, K., Duan, X.-M., Okada, S., Oikawa, H., Nakanishi, H., Vogel, H., Beljonne, D. and Brédas, J.-L., "Fourier analysis of the femtosecond hyper-Rayleigh scattering signal of ionic, fluorescent hemicyanine dyes", J. Opt. Soc. Am. B **17**(2), 256-265 (2000).

[6] Clays, K., Olbrechts, G., Munters, T., Persoons, A., Kim, O.-K. and Choi, L.-S., "Enhancement of molecular hyperpolarizability by supramolecular amylose-dye inclusion complex, studied by hyper-Rayleigh scattering with fluorescence suppression", Chem. Phys. Lett.**293**(5-6), 337-342 (1998).

[7] Pérez-Moreno, J., Asselberghs, I., Zhao, Y., Song, K., Nakanishi, H., Kim, O;-K., Matrai, J., De Maeyer, M., Kuzyk, M. G. and Clays, K., "Combined molecular and supramolecular bottom-up nano-engineering for enhanced nonlinear optical response: experiments, modeling and approaching the fundamental limit", J. Chem. Phys. **126**(7) 074705 (2007).

[8] Reeve, J. E., Collins, H. A., De Mey, K., Kohl, M. M., Thorley, K. J., Paulsen, O., Clays, K. and Anderson, H. L., "Amphiphilic Porphyrins for Second Harmonic Generation Imaging", J. Am. Chem. Soc. 131, 2758-2759 (2009).

[9] Therien, M.J., "How to improve your image", Nature 458, 716-717 (2009).

[10] Nikolenko, V., Nemet, B. and Yuste, R., "A 2-photon and second-harmonic microscope", Methods 30, 3-15 (2003).

[11] Moreaux, C. L., Sandre, O., Blanchard-Desce, M. and Mertus, J., "Membrane imaging by simultaneous second-harmonic generation and two-photon microscopy", Opt. Lett. 25, 320-322 (2000).

[12] Wampler, R. D., Kissick, D. J., Dehen, C. J., Gualtieri, E. J., Grey, J. L., Wang, H. F., Thompson, D. H., Cheng, J. X. and Simpson, G. J., "Selective Detection of Protein Crystals by Second Harmonic Microscopy", J. Am. Chem. Soc. 130, 14076-14077 (2008).

[13] Kobayashi, M., Fujita, K., Kaneko, T., Takamatsu, T., Nakamura, O., Kawata, S.,"Second-harmonic-generation microscope with a microlens array scanner", Opt. Lett. 27, 1324-1326 (2002).

[14] Campagnola, P. J., Millard, A. C., Terasaki, M., Hoppe, P. E., Malone, C. J. and Mohler, W. A., "Three-dimensional high-resolution second-harmonic generation imaging of endogenous structural proteins in biological tissues", Biophys. J. 82, 493-508 (2002).

[15] Khatchatouriants, A., Treinin, M., Chen, Z., Peleg, G., Friedman, N., Bouevitch, O., Rothman, Z., Loew, L. and Sheres, M., "Second-harmonic generation of biological interfaces: Probing the membrane protein bacteriorhodopsin and imaging membrane potential around GFP molecules at specific sites in neuronal cells of C. elegans", Chem. Phys. 245, 133–144 (1999).

[16] Khatchatouriants, A., Lewis, A., Rothman, Z., Loew, L. and Treinin, M., "GFP is a selective non-linear optical sensor of electrophysiological processes in Caenorhabditis elegans", Biophysical Journal 79, 2345-2352 (2000).
[17] Asselberghs, I., Flors, C., Ferrighi, L., Botek, E., Champagne, B., Mizuno, H., Ando, R., Miyawaki, A., Hofkens, J., Van der Auweraer, M. and Clays, K., "Second-Harmonic Generation in GFP-like Proteins," J. Am. Chem. Soc. 130, 15713-15719 (2008).
[18] Pakhomov, A. A. and Martynov, V. I., "GFP Family: Structural Insights into Spectral Tuning", Chemistry & Biology 15, 755-764 (2008).
[19] De Meulenaere, E., Asselberghs, I., de Wergifosse, M., Botek, E., Spaepen, S., Champagne, B., Vanderleyden, J. and Clays, K., "Second-Order Nonlinear Optical Properties of Fluorescent Proteins for Second-Harmonic Imaging", J. Mater. Chem. 19, 7514-7519 (2009).
[20] De Meulenaere, E., de Wergifosse, M., Botek, E., Spaepen, S., Champagne, B., Vanderleyden, J. and Clays, K., "Nonlinear Optical Properties of mStrawberry and mCherry for Second-Harmonic Imaging", J. Nonl. Opt. Phys. Mat. 19, 1-13 (2010).
[21] Cotlet, M., Hofkens, J., Habuchi, S., Dirix, G., Van Guyse, M., Michiels, J., Vanderleyden, J. and De Schryver, F. C., "Identification of different emitting species in the red fluorescent protein DsRed by means of ensemble and single-molecule spectroscopy", Proc. Natl. Acad. Sci. USA 98, 14398-14403 (2001).
[22] Shu, X., Shaner, N. C., Yarbrough, C. A., Tsien, R. Y. and Remington, S. J., "Novel chromophores and buried charges control color in mFruits", Biochemistry 45, 9639–9647 (2006).
[23] Wachter, R. M., Elsliger M. A., Kallio, K., Hanson, G. T. and Remington S. J., "Structural basis of spectral shifts in the yellow-emission variants of green fluorescent proteins", Structure 6, 1267-1277 (1998).
[24] Clays, K., Hendrickx, E., Triest, M., Verbiest, T., Persoons, A., Dehu, C. and Brédas, J.-L., "Nonlinear Optical Properties of Proteins Measured by Hyper-Rayleigh Scattering in Solution", Science 262, 1419-1421 (1993).
[25] Hsu, C. C., Huang, T. H., Zang, Y. L., Lin, J. L., Cheng, Y. Y., Lin, J. T., Wu, H. H., Wang, C. H., Kuo, C. T. and Chen, C. H., "Hyperpolarizabilities of the m-substituent phenyl amine based chromophores determined from the hyper-Rayleigh scattering and two photon absorption induced fluorescence", J. Appl. Phys. 80, 5996-6001 (1996).
[26] Olbrechts, G., Strobbe, R., Clays, K. and Persoons, A., "High-frequency demodulation of multi-photon fluorescence in hyper-Rayleigh scattering", Rev. Sci. Instrum. 69, 2233-2241 (1998).
[27] Clays, K., Wostyn, K., Binnemans, K. and Persoons, A., "Hyper-Rayleigh scattering in the Fourier domain for higher precision: Correcting for multi-photon fluorescence with demodulation and phase data", Rev. Sci. Instrum. 72, 3215-3220 (2001).
[28] Noordman, O. F. J. and van Hulst, N. F., "Time-resolved hyper-Rayleigh scattering: Measuring first hyperpolarizabilities beta of fluorescent molecules", Chem. Phys. Lett. 253, 145-150 (1996).
[29] Olbrechts, G., Wostyn, K., Clays, K., Persoons, A., Kang, S. H. and Kim, K., "Multiphoton fluorescence free hyperpolarizabilities of subphthalocyanines", Chem. Phys. Lett. 308, 173-175 (1999).
[30] Kang, S. H., Kang, Y.-S., Zin, W.-C., Olbrechts, G., Wostyn, K., Clays, K., Persoons, A. and Kim, K., "Novel Columnar Mesogen with Octupolar Optical Nonlinearities: Synthesis, Mesogenic Behavior and Multiphoton-Fluorescence-Free Hyperpolarizabilities of Subphthalocyanines with Long Aliphatic Chains", Chem. Comm. 1999, 1661-1662 (1999).
[31] Olbrechts, G., Wostyn, K., Clays, K. and Persoons, A., "High-frequency demodulation of multiphoton fluorescence in long-wavelength hyper-Rayleigh scattering", Opt. Lett. 24, 403-405 (1999).
[32] Zhang, T.-G., Zhao, Y., Asselberghs, I., Persoons, A., Clays, K. and Therien, M. J., "Design, Synthesis, Linear and Nonlinear Optical Properties of Conjugated (Porphinato)zinc(II)-Based Donor-Acceptor Chromophores Featuring Nitro-thiophenyl and Nitro-oligothiophenyl Electron Accepting Moieties", J. Am. Chem. Soc. 127, 9710-9720 (2005).
[33] Hennrich, G., Murillo, M. T., Prados, P., Al-Saraierh, H., Georghiou, P. E., Thompson, D. W., Asselberghs, I. and Clays, K., "Alkynyl Expanded Donor-Acceptor Calixarenes: Geometry and Second-Order Nonlinear Optical Properties", Chem. Eur. J. 13, 7753-7761 (2007).
[34] Duncan, T. V., Song, K., Hung, S.-T., Miloradovic, I., Nayak, A., Persoons, A., Verbiest, T., Therien, M. J. and Clays, K., "Molecular Symmetry and Solution Phase Structure Interrogated by Hyper-Rayleigh Depolarization Measurements: Insights for Elaborating Highly Hyperpolarizable D_2-Symmetric Chromophores", Ang. Chem. Int. Ed. 47, 2978-2981 (2008).
[35] Oudar, J. L. and Chemla, D. S., "Hyperpolarizabilities of Nitroanilines and Their Relations to Excited-State Dipole-Moment", J. Chem. Phys. 66, 2664-2668 (1977).